Response to Reviewer Comments

In this manuscript, Song, Zhang, and Yan mapped the future afforestation distribution of China under political guidance and climate change. It is a good example to serve the society using numerical techniques. Overall, this manuscript is clear-written, easy to understand, and seems to be methodologically sound. I like the most of plots in this manuscript. However, I still have several comments that should be addressed below.

Response: We thank the reviewer for all the constructive comments provided. These comments are valuable and very helpful for revising and improving our paper. We have studied the comments carefully and have made revisions to the revised version. I hope these major revisions meet with approval. The point-by-point responses to the reviewer's comments are as follows:

Specific comments:

Line 20: Please explain the Hu Line. Readers outside are not familiar with this geographical division.

Response: We have added the explanation in the abstract as follows:

The newly afforestation grid cells would be located around and to the east of the Hu Line (a geographical division line stretching from Heihe to Tengchong).

We have added the details in the results as follows:

Hu Line, a geographical division line of climate zone, and population density, economic development in China, stretches from Heihe to Tengchong.

Line 24: Replace "surface climate" with "surface hydroclimate regime".

Response: It is revised.

Line 29: Afforestation not only influences the land surface energy and mass budgets, but also affects the water cycle. Water cycle should be mentioned, since in the main text PRCP and ET are analyzed.

Response: We have added it as follows:

Forests change the surface energy, mass budgets, and water cycle by modifying the physical

properties of the land surface, such as albedo and roughness.

Lines 27-32: The authors listed several papers describing the benefits of afforestation. More details would be helpful for readers to understand the impacts of afforestation from the process level.

Response: We have included the details as follows:

Afforestation could increase carbon stocks in terrestrial ecosystems by absorbing atmospheric carbon dioxide through its biogeochemical effect (Jayakrishnan et al., 2023; Zhu et al., 2019; Gundersen et al., 2021). Meanwhile, afforestation changes the surface energy, mass budgets, and water cycle by modifying the physical properties of the land surface, such as albedo and roughness, and the partitioning between sensible and latent heat fluxes through biogeophysical progress as well (Bonan, 2008; Breil et al., 2021; Wang et al., 2023). Specifically, afforestation causes warming effects due to the decreased albedo and cooling effects due to increased evapotranspiration, which can partly offset or amplify the cooling effects due to taking up carbon from the atmosphere.

Line 33: "Aggressively" is not a positive word.

Response: We have deleted it.

Line 36: Add the time constraint for global greening.

Response: We have included it. "China's total forest cover has increased from 8.6 % in 1949 to 24.02 % in 2022 (Zhang and Song, 2006; Fu et al., 2023; Moore et al., 2016), resulting in a 42% contribution to the greening in China during 2000-2017 (Chen et al., 2019)."

Line 44: Please refine this sentence: "trigger consequent effects on climate change, hydrological processes, carbon budget, ecosystem services".

Response: We agree that this sentence is difficult to understand. We have refined it as follows:

Such large-scale afforestation in the future would modify the land cover conversions from non-forestland to forestland. These conversions could cause consequent effects on climate change (Wang et al., 2023), hydrological processes (Tian et al., 2022), carbon budget (Maneke-Fiegenbaum et al., 2021), ecosystem services (Wang and Li, 2022), etc.

References

Wang, H., Yue, C., & Luyssaert, S. (2023). Reconciling different approaches to quantifying land surface temperature impacts of afforestation using satellite observations. Biogeosciences, 20(1), 75-92.

Maneke-Fiegenbaum, F., Santos, S. H., Klemm, O., Yu, J. C., Chiang, P. N., & Lai, Y. J. (2021). Carbon dioxide fluxes of a young deciduous afforestation under the influence of seasonal precipitation patterns and frequent typhoon occurrence. Journal of Geophysical Research: Biogeosciences, 126(2), e2020JG005996.

Tian, L., Zhang, B., Chen, S., Wang, X., Ma, X., & Pan, B. (2022). Large-scale afforestation enhances precipitation by intensifying the atmospheric water cycle over the Chinese Loess Plateau. Journal of Geophysical Research: Atmospheres, 127(16), e2022JD036738.

Wang, Y., & Li, B. (2022). Dynamics arising from the impact of large-scale afforestation on ecosystem services. Land Degradation & Development, 33(16), 3186-3198.

Line 45-46: Please provide the details for "sensitive to wetland reduction caused by afforestation" and "properties and intensities of these effects are highly dependent on the afforestation location and area. " I left confused about how the authors conclude.

Response: Thank you for your suggestion. We replaced an example as follows:

It is crucial that the effects of afforestation are highly dependent on the afforestation location and area. For example, tropical afforestation leads to greater cooling effects than boreal afforestation (Arora and Montenegro, 2011). Therefore, it is urgent to arrange the national planned afforestation area to specific areas and project the possible land cover changes due to afforestation.

Reference

Arora, V. K., & Montenegro, A. (2011). Small temperature benefits provided by realistic afforestation efforts. Nature Geoscience, 4(8), 514-518.

Line 49-55: The authors listed several papers and did not explain their findings on climate impact; in addition, please identify the deficiency of "employ idealistic and hypothetical

afforestation scenarios".

Response: We have added the findings on climate impact as follows:

Odoulami et al. (2019) fully replaced the savanna areas (between 8°N and 12°N) with evergreen broadleaf trees over West Africa to investigate the climate effects of future afforestation. The obvious increase in the total annual precipitation was found over the afforested area. Similarly, Abiodun et al. (2013) employed random afforestation options to replace 25 %–100 % of the current land cover in Nigeria and found a local cooling effect induced by afforestation.

The deficiency of "employ idealistic and hypothetical afforestation scenarios" is that the afforestation scenarios were set by the authors themselves, and both the national afforestation plan and the future climate change constraint are neglected.

Lines 63-71: Besides the dynamic downscaling, it would be beneficial to discuss the statistical downscaling. Moreover, dynamic vegetation studies for future projections in China are relevant to this topic, and the related studies should be mentioned in the literature review.

Response: Following your suggestion, we will restructure it. We have added the dynamic vegetation and statistical downscaling studies in the revised manuscript as follows:

For statistical downscaling, the revision in the introduction is as follows:

However, the resolution of the raw GCM is much coarser (~100 km–300 km) to describe the fine land surface features at the regional scale (Varney, 2022; Turner et al., 2023; Song and Yan, 2022; Parsons, 2020). To overcome such shortage, downscaling techniques are widely used to translate GCM output to high-resolution data. Statistical downscaling involves the establishment of statistical relationships between local climate variables and large-scale atmospheric fields (Wilby and Wigley, 1997). However, it is not clear whether this historical statistical relationship is always stable in future periods. Statistical downscaling cannot ensure the physical consistency among meteorological variables. In contrast, the physically-based dynamic downscaling using a regional climate model (RCM) nested within a GCM could provide high-resolution climate simulations (Giorgi and Mearns, 1999; Mishra et al., 2014). The physical consistency is crucial to identify potential afforestation regions due to the multiple meteorological variables involved. Previous studies (Liu et al., 2020; Bowden et al., 2021) have employed the dynamical downscaling approach to quantify the climatological suitability for each nature vegetation type.

For statistical downscaling, the revision in the discussion is as follows:

Although the resolution of our dynamic downscaled simulation (25 km) is finer than raw GCMs (~100 km), it is difficult to meet the needs of afforestation planning in areas with complex topography. Convection-permitting climate modelling at the kilometre-scale has recently been developed to reproduce better mesoscale atmospheric processes (Prein et al., 2015; Lucas-Picher et al., 2021), and obviously improve the WRF simulation, especially precipitation (Knist et al., 2020). However, increasing the resolution of the simulation implies higher computational costs. In contrast, statistical downscaling methods are also known to obtain high-resolution climate data with few computational resources (Tang et al., 2016). The multi-model ensemble means from statistical downscaling CMIP6 can significantly reduce the biases compared to individual models (Gebrechorkos et al., 2019). Thus, some statistically downscaled CMIP6 datasets (Gebrechorkos et al., 2023; Lin et al., 2023; Thrasher et al., 2022), with a resolution of 0.1°-0.25° covering the global land, can be applied to explore the future global potential afforestation area in following work. However, it is noted that the statistically downscaling data may have a limitation, as the covariance among the variables may not align with physical laws.

For dynamic vegetation, the revision in the introduction is as follows:

In addition, process-based dynamic global vegetation models (DGVMs) are also useful tools to help quantify future afforestation scenarios (Krinner et al., 2005; Horvath et al., 2021). The DGVMs (i.e., LPJ-GUESS) have commonly been applied to explore the responses of potential natural vegetation distribution to climate change (Hickler et al., 2012; Verbruggen et al., 2021). The DGVMs driven by meteorological data generally consider complex biogeophysical, biogeochemical, and physiological progress, such as evapotranspiration, carbon–nitrogen interactions, photosynthesis, and so on (Cramer et al., 2001). Given that both model process parameters and future meteorological data from GCMs represent a large source of uncertainty in DGVMs, the double overlap can lead to great uncertainties (Jiang et al., 2012; Martens et al., 2021).

Reference

Hickler, T., Vohland, K., Feehan, J., Miller, P. A., Smith, B., Costa, L., et al. (2012). Projecting the future distribution of European potential natural vegetation zones with a generalized, tree species-based dynamic vegetation model. Global Ecology and Biogeography, 21(1), 50-63.

Krinner, G., Viovy, N., de Noblet-Ducoudré, N., Ogée, J., Polcher, J., Friedlingstein, P., et al. (2005). A dynamic global vegetation model for studies of the coupled atmosphere-biosphere system. Global Biogeochemical Cycles, 19(1).

Jiang, Y., Zhuang, Q., Schaphoff, S., Sitch, S., Sokolov, A., Kicklighter, D., & Melillo, J. (2012). Uncertainty analysis of vegetation distribution in the northern high latitudes during the 21st century with a dynamic vegetation model. Ecology and Evolution, 2(3), 593-614.

Martens, C., Hickler, T., Davis-Reddy, C., Engelbrecht, F., Higgins, S. I., Von Maltitz, G. P., et al. (2021). Large uncertainties in future biome changes in Africa call for flexible climate adaptation strategies. Global Change Biology, 27(2), 340-358.

Horvath, P., Tang, H., Halvorsen, R., Stordal, F., Tallaksen, L. M., Berntsen, T. K., & Bryn, A. (2021). Improving the representation of high-latitude vegetation distribution in dynamic global vegetation models. Biogeosciences, 18(1), 95-112.

Verbruggen, W., Schurgers, G., Horion, S., Ardö, J., Bernardino, P. N., Cappelaere, B., et al. (2021). Contrasting responses of woody and herbaceous vegetation to altered rainfall characteristics in the Sahel. Biogeosciences, 18(1), 77-93.

Giorgi, F., & Mearns, L. O. (1999). Introduction to special section: Regional climate modeling revisited. Journal of Geophysical Research, 104(D6), 6335–6352. https://doi.org/10.1029/98JD02072

Cramer, W., Bondeau, A., Woodward, F. I., Prentice, I. C., Betts, R. A., Brovkin, V., et al. (2001). Global response of terrestrial ecosystem structure and function to CO2 and climate change: results from six dynamic global vegetation models. Global change biology, 7(4), 357-373.

Prein, A. F., Langhans, W., Fosser, G., Ferrone, A., Ban, N., Goergen, K., et al. (2015). A review on regional convection-permitting climate modeling: Demonstrations, prospects, and challenges. Reviews of Geophysics, 53(2), 323-361.

Lucas-Picher, P., Argüeso, D., Brisson, E., Tramblay, Y., Berg, P., Lemonsu, A., et al. (2021). Convection-permitting modeling with regional climate models: Latest developments and next steps. Wiley Interdisciplinary Reviews: Climate Change, 12(6), e731.

Knist, S., Goergen, K., & Simmer, C. (2020). Evaluation and projected changes of precipitation statistics in convection-permitting WRF climate simulations over Central Europe. Climate Dynamics, 55(1-2), 325-341.

Tang, J., Niu, X., Wang, S., Gao, H., Wang, X., & Wu, J. (2016). Statistical downscaling and dynamical downscaling of regional climate in China: Present climate evaluations and future climate projections. Journal of Geophysical Research: Atmospheres, 121(5), 2110-2129.

Wilby, R. L., & Dawson, C. W. (2013). The statistical downscaling model: insights from one decade of application. International Journal of Climatology, 33(7), 1707-1719.

Gebrechorkos, S., Hülsmann, S., & Bernhofer, C. (2019). Regional climate projections for impact assessment studies in East Africa. Environmental Research Letters, 14(4), 044031.

Gebrechorkos, S., Leyland, J., Slater, L., Wortmann, M., Ashworth, P. J., Bennett, G. L., et al. (2023). A high-resolution daily global dataset of statistically downscaled CMIP6 models for climate impact analyses. Scientific Data, 10(1), 611.

Lin, H., Tang, J., Wang, S., Wang, S., & Dong, G. (2023). Deep learning downscaled high-resolution daily near surface meteorological datasets over East Asia. Scientific Data, 10(1), 890.

Thrasher, B., Wang, W., Michaelis, A., Melton, F., Lee, T., & Nemani, R. (2022). NASA global daily downscaled projections, CMIP6. Scientific Data, 9(1), 262.

Line 67: Please talk about the uncertainties for GCMs.

Response: Following your suggestion, we will restructure the discussion. We have added it as follows:

This study may have some limitations and uncertainties. Following the approach of existing studies (Ma et al., 2023; Qiu et al., 2022), we also utilize the bias-correction LBC in dynamical downscaling. However, the model uncertainty in the future climate projection is difficult to quantify because one GCM is used to nest into the WRF model. The projected result generally exhibits variations based on the choice of driving GCMs (Gao et al., 2022). This divergence can be attributed to the inherent configurations and physics parameterization of the GCMs, distinct radiative forcing scenarios, and varying equilibrium climate sensitivities found in CMIP6 models (Zuo et al., 2023; Bukovsky and Mearns, 2020). For instance, the high emissions scenario could lead to higher temperature and stronger precipitation in China (Yang et al., 2021). Consequently, the suitability of land for future forests may change accordingly. Exploring the impacts of different SSPs on the distribution of potential afforestation regions would be an intriguing avenue for future research. To address the concerns on model uncertainty, using WRF forced by multiple bias-correction CMIP6

model can explore the source of uncertainty, and the ensemble means for downscaled climate simulation would help to obtain a more robust projection. In addition, the different combinations of physics parameterization schemes in the WRF model also influence the simulation performance (Gbode et al., 2019). Selecting the optimal combination is beneficial for reducing underlying bias.

References

Ma, M., Tang, J., Ou, T., & Zhou, P. (2023). High-resolution climate projection over the Tibetan Plateau using WRF forced by bias-corrected CESM. Atmospheric Research, 286, 106670.

Qiu, Y., Feng, J., Yan, Z., Wang, J., & Li, Z. (2022). High-resolution dynamical downscaling for regional climate projection in Central Asia based on bias-corrected multiple GCMs. Climate Dynamics, 58(3-4), 777-791.

Gao, S., Zhu, S., & Yu, H. (2022). Dynamical downscaling of temperature extremes over China using the WRF model driven by different lateral boundary conditions. Atmospheric Research, 278, 106348.

Zuo, Z., Fung, J. C., Li, Z., Huang, Y., Wong, M. F., Lau, A. K., & Lu, X. (2023). Projection of future heatwaves in the Pearl River Delta through CMIP6-WRF dynamical downscaling. Journal of Applied Meteorology and Climatology, 62(9), 1297-1314.

Bukovsky, M. S., & Mearns, L. O. (2020). Regional climate change projections from NA-CORDEX and their relation to climate sensitivity. Climatic Change, 162(2), 645-665.

Yang, X., Zhou, B., Xu, Y., & Han, Z. (2021). CMIP6 evaluation and projection of temperature and precipitation over China. Advances in Atmospheric Sciences, 38, 817-830.

Gbode, I. E., Dudhia, J., Ogunjobi, K. O., & Ajayi, V. O. (2019). Sensitivity of different physics schemes in the WRF model during a West African monsoon regime. Theoretical and Applied Climatology, 136, 733-751.

Lines 79-80: please add sequence numbers for three categories.

Response: We have added it as follows:

This study used three categories of data: (1) ground meteorology measurements data, satellite-observed land use/cover data, (2) national planned afforestation area data, (3) climate modelling data from GCM, and ERA5 reanalysis data.

Figure 2: The red text on a dark blue background is hard to read.

Response: We changed it from red to white to make it easier to read.

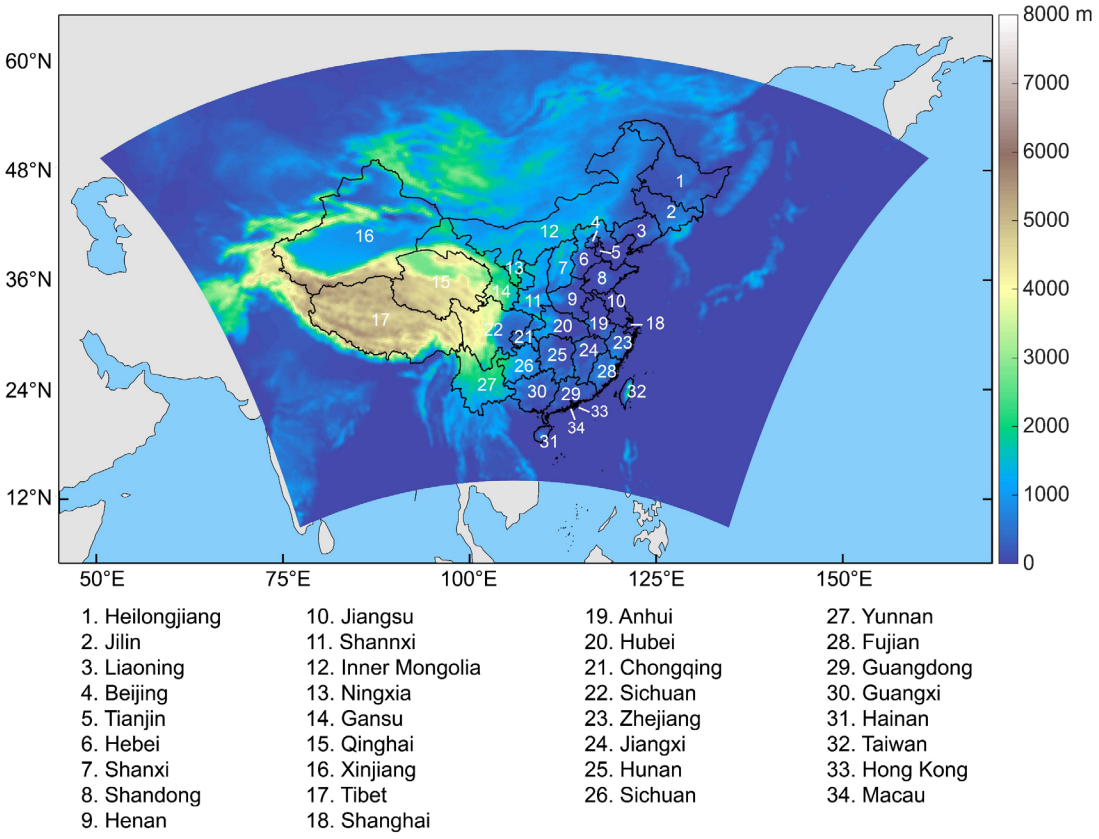

Figure 1: Model domain with topography. The black boundaries indicate each province in China.

Lines 162-163: Did the authors test whether the model has reached the equilibrium state with only one year of spinning up?

Response: The spin-up time of the WRF model is important to reach the physical equilibrium state and to avoid inhomogeneities. Its length is determined by the quality of initial conditions inputs. In this study, we use the ERA5 reanalysis data and the MPI–ESM1–2–HR model as the initial conditions. They generally reach the equilibrium state in a short time due to the physical consistency between the variables. Previous studies have demonstrated that 4- to 8-day for atmospheric variables and 1-year spin-up time for soil moisture and temperature is enough (Zhong et al., 2007; Katragkou et al., 2015). Therefore, the model can reach the equilibrium state in this study.

Reference

Gao, S., Huang, D., Du, N., Ren, C., & Yu, H. (2022). WRF ensemble dynamical downscaling of precipitation over China using different cumulus convective schemes. Atmospheric Research, 271, 106116.

Tang, J., Lu, Y., Wang, S., Guo, Z., Lu, Y., & Fang, J. (2023). Projection of hourly extreme precipitation using the WRF model over eastern China. Journal of Geophysical Research: Atmospheres, 128(1), e2022JD036448.

Zhong, Z., Yijia, H. U., Jinzhong, M. I. N., & Honglei, X. U. (2007). Numerical experiments on the spin-up time for seasonal-scale regional climate modeling. Journal of Meteorological Research, 21(4), 409–419.

Katragkou, E., García Díez, M., Vautard, R., Sobolowski, S. P., Zanis, P., Alexandri, G., Cardoso, A., Colette, A., Fernandez, J., Gobiet, A., Goergen, K., Karacostas, T., Knist, S., Mayer, S., Soares, P. M. M., Pytharoulis, I., Tegoulias, I., Tsikerdekis, A., & Jacob, D. (2015). Regional climate hindcast simulations within EURO-CORDEX: Evaluation of a WRF multi-physics ensemble. Geoscientific Model Development, 8(3), 603–618.

Line 164: Delete the space between FUT_ and MPI.

Response: We have deleted it.

Line 212: Please change the unit mu into a standard international unit.

Response: We have changed "1.825 billion mu" to "121.67×10^4 km^2 ".

Figure 3: in addition to the difference in FigS2. A pattern correlation and RMSE for AT, TP, and PE in Fig.3 would be beneficial.

Response: We have added it to the supplementary material.

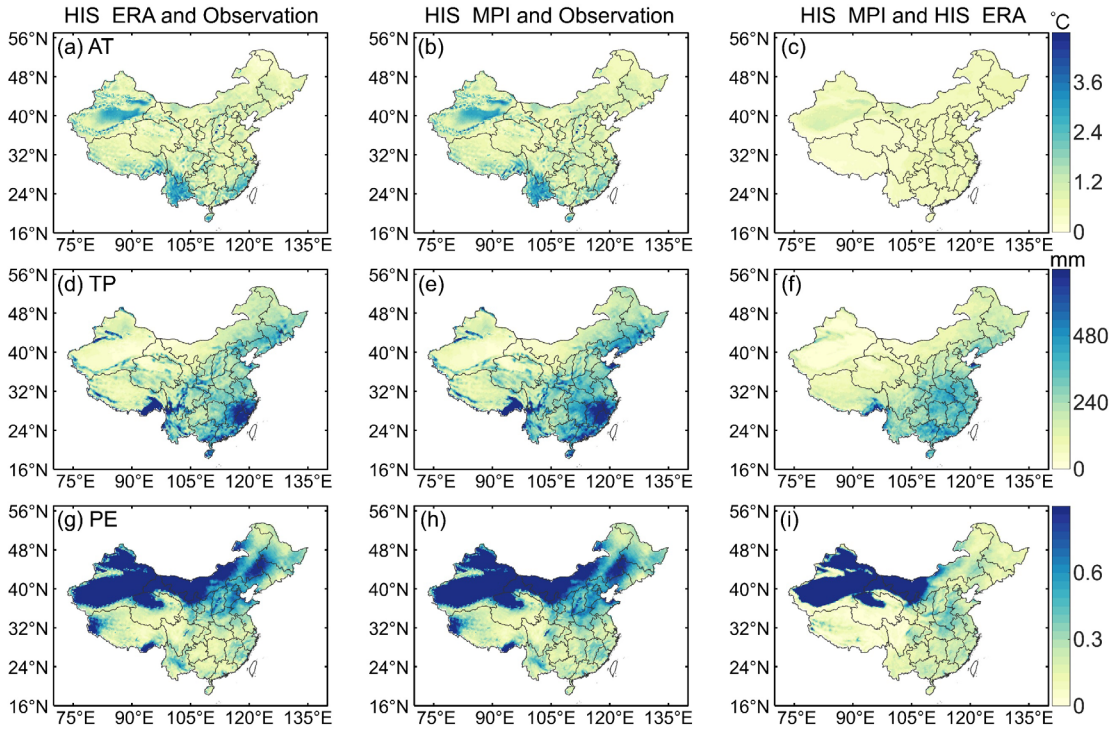

Figure 2: Comparison of observation, HIS_ERA and HIS_MPI based on RMSE. HIS_ERA and HIS_MPI indicate the WRF simulation driven by ERA5 reanalysis data and bias-corrected MPI–ESM1–2–HR model, respectively. The observation derives from the CN05.1 dataset.

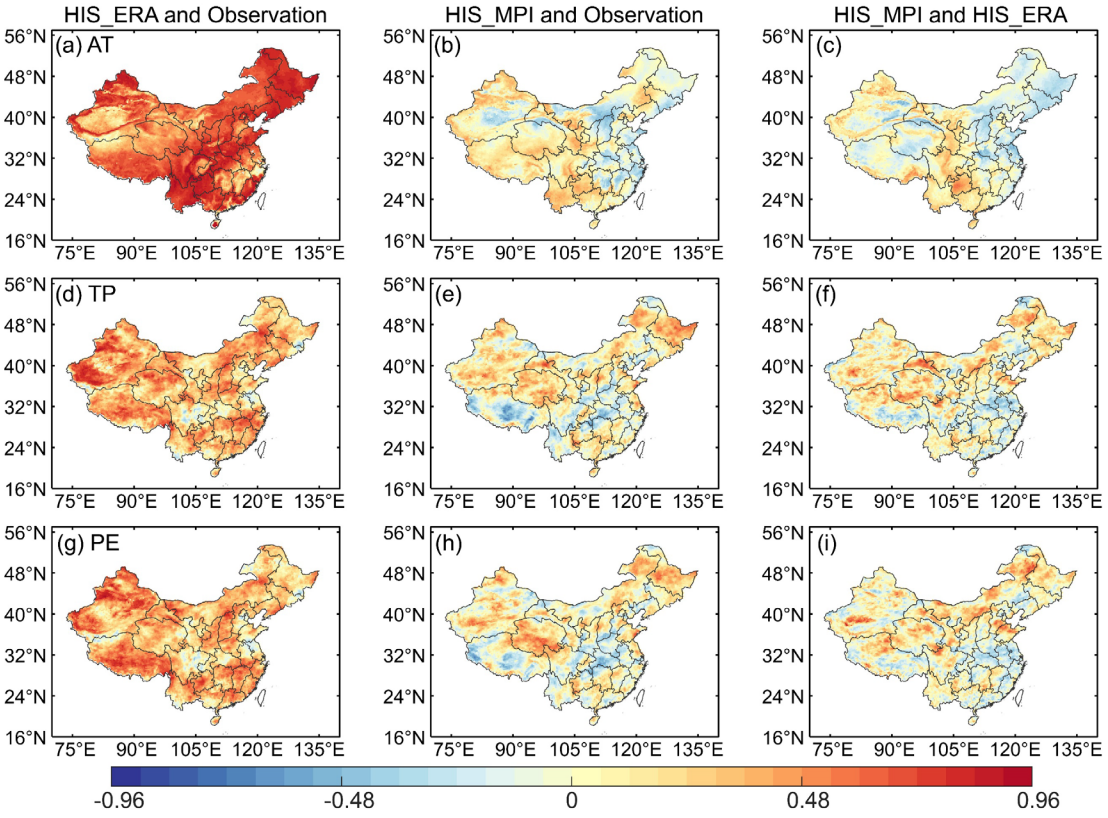

Figure 3: Comparison of observation, HIS_ERA and HIS_MPI based on spatial correlation coefficient. HIS_ERA and HIS_MPI indicate the WRF simulation driven by ERA5 reanalysis data and bias-corrected MPI–ESM1–2–HR model, respectively. The observation derives from the CN05.1 dataset.

Figure 4: Maybe I missed something, but adding texts to identify the difference among a, b, and c would be helpful. More info in the caption also would be beneficial for reader to understand this figure. One interesting finding from the figure is that the model tends to underestimate the TP in the high value (>1600 mm) category and overestimate the PE in the high value (>3; unit?) category.

Response: We have added more information to the caption of Figure 4. " Figure 4: Scatterplots of the annual average biotemperature (AT), annual total precipitation (TP), and potential evapotranspiration ratio (PE) for each grid against the observation and HIS_ERA, observation and HIS_MPI, HIS_MPI, and HIS_ERA. HIS_ERA and HIS_MPI indicate the WRF simulation driven by ERA5 reanalysis data and the bias-corrected MPI–ESM1–2–HR model, respectively. The observation derives from the CN05.1 dataset. Evaluation indexes included the bias, mean absolute error (MAE), and spatial correlation coefficient (R). The black dotted line indicates a 1:1 line."

We find that the simulated TP exceeding 1600 mm in southern China is underestimated and the simulated PE exceeding 3 in northwest China is overestimated. The WRF model generally overestimates light rain, and underestimates heavy rain, especially extreme precipitation (Mugume et al, 2018). Therefore, it is necessary to further improve the simulation accuracy of the WRF model.

Reference

Mugume, I., Basalirwa, C., Waiswa, D., Nsabagwa, M., Ngailo, T. J., Reuder, J., & Semujju, M. (2018). A comparative analysis of the performance of COSMO and WRF models in quantitative rainfall prediction. International Journal of Marine and Environmental Sciences, 12(2), 130-138.

Figure 5: Please add some values for change in the Fig. 5b.

Response: The flow diagram was improved and specific values are included.

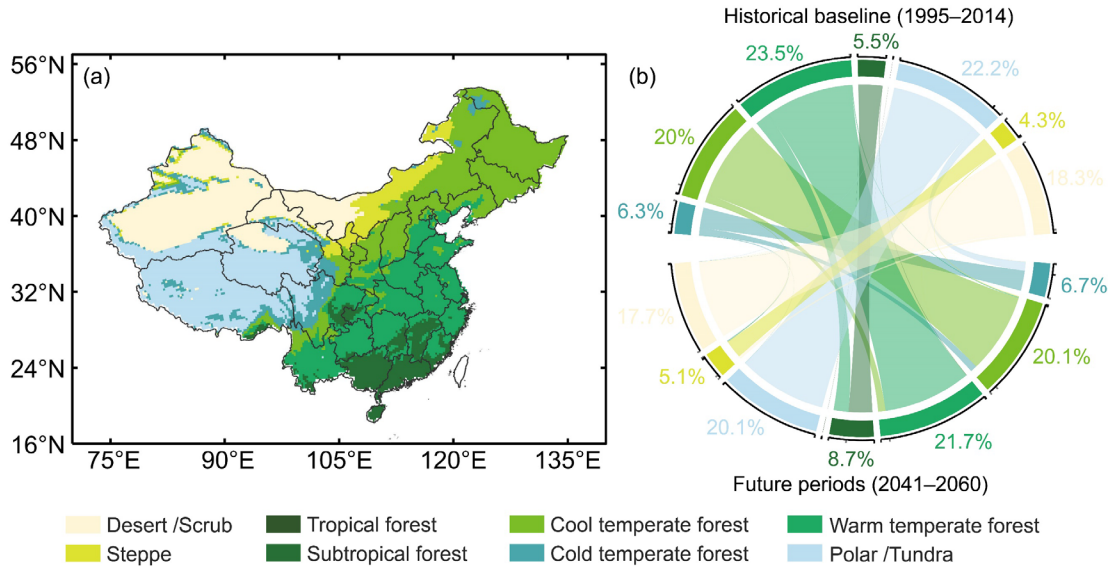

Figure 4: Projected spatial pattern of (a) potential vegetable types from HLZ model under the SSP2–4.5 scenario in the future periods (2041–2060) from the FUT_ MPI simulation, and (b) area changes across historical baseline (1995–2014) and future periods, where the calculations are based on FUT_ MPI simulation versus HIS_ MPI simulation.

Figure 6: Some text overlaps with the map.

Response: We have changed it.

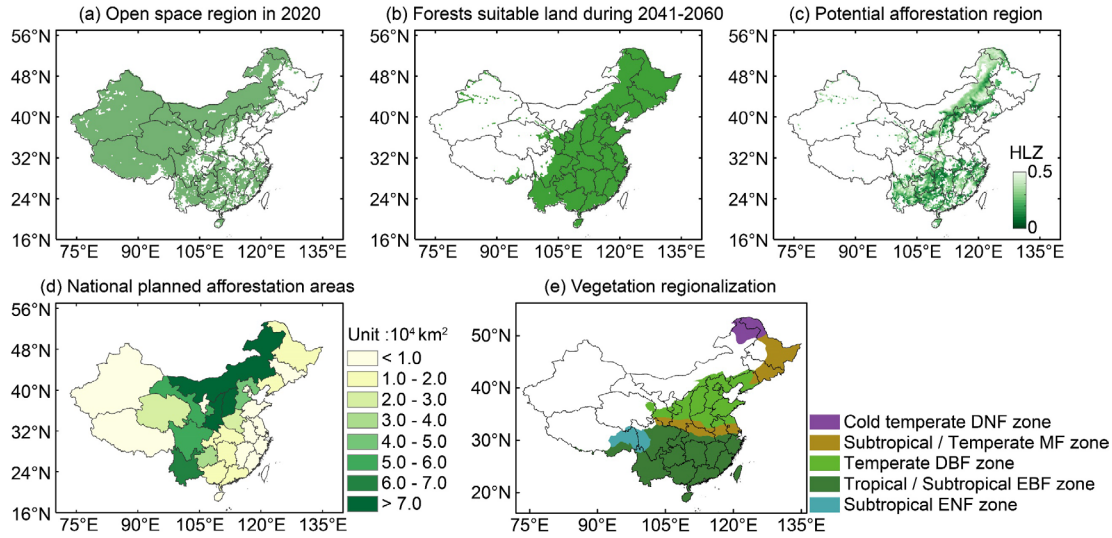

Figure 5: Spatial distribution of (a) historical open space region for afforestation, (b) future potential forestation domain (PFD) from HLZ model considered as the forest suitable lands, (c) potential afforestation region constrained by climate change, (d) national planned afforestation areas in the individual provinces from the NFMP, (e) Chinese vegetation regionalization map.